

Aleksandar Saljnikov

Associate Professor
University of Belgrade
Faculty of Mechanical Engineering

Milan Gojak

Assistant Professor
University of Belgrade
Faculty of Mechanical Engineering

Miroslav Trifunović

Innovation Center Researcher
University of Belgrade
Faculty of Mechanical Engineering

Srdan Andrejević

Doctoral Course Student
University of Belgrade
Faculty of Mechanical Engineering

Mirko Dobrnjac

Assistant Professor
University of Banjaluka
Faculty of Mechanical Engineering

Research on Infrared Emission Spectra of Pulverized Coal Ash Deposits

This paper deals with thermal radiation properties of ash deposits on a pulverized coal boiler of an electric power plant. Normal emittance spectra in the 2.5-25 μm interval, and total normal emittance, were measured on 2 kinds of ash layers of a mm magnitude order thickness, at 560→1460→560 K in heating and cooling. The emittance increases with ash radiation wavelength and temperature. Ash powder is sintered and fused above 1200 K. The emittance of the sintered layer is above that of the unsintered layer. The authors propose, and explain by example, correlating the experimentally obtained emittance spectra of ash deposits with a continuous curve, the formula of which defines the dependence of the emittance on wavelength and temperature, i.e. $\epsilon = \epsilon(\lambda, T)$. Use of this formula, with parameter values determined by the proposed methodology, may greatly simplify the practical application of the experimentally determined emittances in the thermal design of existing and new steam boiler furnaces.

Keywords: thermal radiation, spectroscopy, coal ash deposit, temperature, wavelength.

1. INTRODUCTION

In thermal design of a power plant boiler, in which pulverized low quality coal is used as the fuel, knowledge of thermal radiation characteristics of ash is important, since flying ash is deposited on the boiler walls and decreases the power plant boiler efficiency.

Ash deposits are non-metallic materials. Thermal radiation characteristics of such materials greatly differ from those of metallic walls of the furnace, i.e. the surfaces of heat exchanger pipes in the boiler furnace. The real surfaces, by their non-homogeneity and structure, differ from the ideal surfaces as well – it is practically impossible to quantify the influence that deposits exert upon the heat transfer, using the analytic tools. Therefore, this problem is often solved by using the experimental methods in order to determine the thermal radiation characteristics of deposits, concretely – their emittance and (less often) their absorptance.

There have been several works done on thermal radiation characteristics of ash deposits. Boov and Goard [1,2] described their research for determining emittance of deposits formed in lignite combustion at temperatures up to 1450 K. The measurement of total hemispherical emittance was done at 550-1450 K in the $\lambda=0.13-9.5$ wavelength range, and of a spectral value at $\lambda=0.9 \mu\text{m}$. It was concluded, and later confirmed by other authors [3,4,5,8], that the analyzed quantities strongly depend upon temperature and on the thermal history of the material. It was observed (see Fig.1) that ϵ^{tot} decreases from 0.86 (at 550 K) down to 0.58 (at 1200-1300 K). The following temperature increase

(1300-1450 K), leads to sintering and later fusion of ash deposits, ϵ^{tot} starts to increase and reaches ≈ 0.75 (at ≈ 1450 K). In cooling, ϵ^{tot} does increase continually, to ≈ 0.88 (at ≈ 560 K).

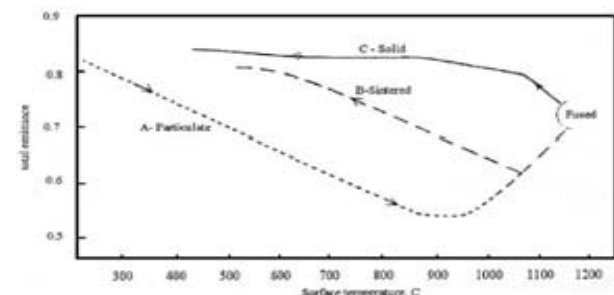


Figure 1. Ash total emittance vs. temperature [1]

To relate radiative properties and heat conductance of deposits with physical and chemical properties, observed or measured, a review [3] was made. The liaison between the theory and real data was analyzed for the first time, i.e. spectra of the real indices of refraction and absorption, measured at room temperature for 4 synthetic materials, composition similar to real slag [4]. Spectral absorptance was determined from experimental data (by Mie theory) and the total emittance of ash particles, as well.

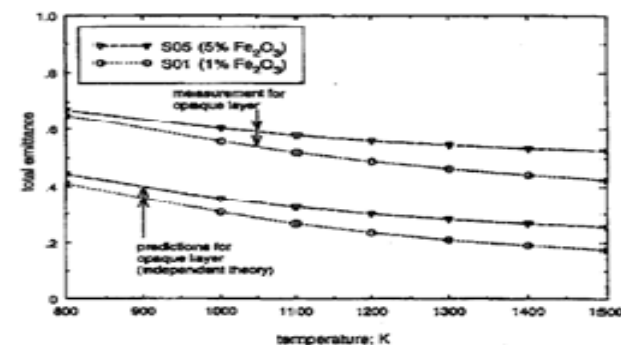


Figure 2. Measured and predicted ash emittance [5]

Received: May 2012, Accepted: June 2012
Correspondence to: Dr Aleksandar Saljnikov
Faculty of Mechanical Engineering,
Kraljice Marije 16, 11120 Belgrade 35, Serbia
E-mail: asaljnikov@mas.bg.ac.rs

The authors of article [5] have presented their own experimental and analytical results showing the influence that the dependent effects (scattering and absorption are called dependent effects if these phenomena of a particle in a medium are affected by the neighbouring particles) exert upon the determination of the ash deposit emittance. In that paper a model is outlined – for determining the spectral emittance (directional, normal & hemispherical) of semi-transparent and opaque deposits that deliberately does not consider the dependent effects. The predictions illustrate the influence that particle size and chemical composition exert upon emittance of coal ash deposits.

While both the measured and the predicted values of total hemispherical emittance of the deposits are apart by approximately the same value, attributed to the chemical composition, the difference between the measured total emittance values and the predicted values (by virtue of non-dependent theory) was pronounced (Fig.2) especially for more transparent materials. Apparently, in these plots there is no „hysteresis“ characteristic for the experiments performed when doing research on these phenomena (e.g. in [1,4,8,10]). This is because, for simplicity, the authors had considered the deposit in its already sintered and fused state – realistic for hotter furnaces.

Considering the here outlined research, the following point deserves to be focused onto. The thermal radiation properties of ash deposits are temperature dependent. Spectral behavior of ash deposit is the main cause of the strong temperature dependence of total emittance. Data on emittance of Serbian (and other as well) lignites and their ashes are scarce. These data are considered to find themselves among the main parameters in steam boiler design (in thermal power plants and fruit and vegetables drying), so the present authors undertook research on thermal radiation properties of Serbian coal ash.

Spectral normal emittance (in 2.5-25 μm range) and total normal emittance were measured on 2 kinds of ash layers of a mm order thickness, at 560-1460-560 K in heating and cooling. Their dependence on λ and T , and upon ash sintering and fusion, was studied. The authors propose, and do explain by an example, correlating the experimentally obtained emittance spectra by continuous function that defines the dependence of ϵ on λ and T . This might greatly simplify the practical applications of the experimentally determined emittances within the thermal design of existing and new steam boiler furnaces.

2. EXPERIMENTAL PROCEDURE

2.1 Materials of specimens

Materials of the specimens are broken pieces of flying ash deposits on a boiler furnace heat exchange surfaces of a power plant in Serbia, where pulverized lignite coal is combusted. These pieces were sampled at two positions along the furnace height as shown in Table 1.

The materials are the inorganic compounds that were solidified like rocks with inhomogeneities of an order of mm. The pieces were powdered manually and the layers

of sampled pieces are prepared. The average properties of powdered ash layers were investigated in the experiments, that are specified in detail later in the text.

Table 1. Specification of ash deposit specimens

	height in furnace	structure	color		ρ_p kg/m ³
			bulk	powder	
1	10m, in-clin wall	s-granul	brown	pink	1378
		i-layer	darkred		
2	30m, rear wall	s-granul	brown	brown	1469
		i-layer	black		

Table 1 shows the specification of the ash specimens, where ρ_p is the heaping mass density. Table 2 presents the chemical composition of the same two ash specimens.

Table 2. Chemical composition of ash specimens (wt.%)

	No.1	No.2
CaSO ₄	48.2	25.9
CaO	4.7	18.9
Al ₂ O ₃	3.1	3.4
FeO	29.4	35.3
SiO ₂	7.4	9.5
others	7.2	7.0

2.2 Ash specimen layers

Powder of an ash specimen is set in a vessel of the stainless steel JIS-SUS304 (of 1, 3 or 5 mm in depth) to form a specimen layer [9]. A K-type thermocouple was welded on the rear surface of the vessel for temperature control of the specimen layer. Temperature of the layer was measured by a K-thermocouple of 100 μm diameter. The hot-junction of thermocouple is set at a position of 0-0.5 mm depth by lightly pressing it into the layer. The specimen layer is radiation-heated from the back by four silicon carbide rod heaters. A water-cooled Cu radiation shield has been located at the very surroundings of the powdered ash deposit specimen surface, so that the radiation emitted by hot surroundings of the specimen is not multiply reflected and does not reach and affect the optical measuring system.

The specimen layer is heated up to ≈ 560 K by heating rate of 2 K/min, common for similar experiments, and optical measurement is made. Heating is continued at the same rate – at each 100 K up to ≈ 1460 K similar optical measurement is done. The value of maximal temperature was chosen because, it is common [1,3] that ash of the similar chemical composition and size is yet sintered and fused (molten) – before reaching it. (This coincides with observations on cooled-down specimens.) At reaching the maximum temperature, the specimen is cooled down with the cooling rate of 2 K/min and, at every 100 K down to ≈ 560 K, optical measurement is repeated.

2.3 Optical measurement

At each 100 K, the movable mirror is displaced out of the observation area of the spectrophotometer, which [9] accepts the specimen radiation flux within the solid

angle at zenith angle of $\pm 10^\circ$, the (a) measurement is done; then the movable mirror is slid above the specimen to the position for (b) measurement, and it is done by redirecting the same radiation flux to the total radiation fluxmeter.

Emissance of specimen ash layers is measured by a comparison method in which the radiation emitted from the specimen surface is compared with that emitted from the reference blackbody. The spectrophotometer, that is being utilized for the infrared spectral measurement, is Fourier transformation type (Shimadzu Co., FTIR-4200, [6]), which monitors the spectrum of 1868 wavelength points in the region of wavelengths $\lambda=2.5-25 \mu\text{m}$, where more than 95 % and 75 % of radiation energy of the blackbody at temperatures of 560 K and 1460 K are covered, respectively. Spectral resolution of the FTIR spectrophotometer is 2 cm^{-1} at $\lambda=12.3 \mu\text{m}$, which is rather too fine for heat transfer research. Total radiation flux meter for the total emittance measurement is a modified radiation type pyrometer (Minolta Co., 505S, [7]), which senses the infrared radiation by a thermoelectric detector via two non-coated Al mirrors and a KRS-5 window. Spectral absorption characteristics of the mirrors and the window are checked to be gray enough over $\lambda=1-40 \mu\text{m}$ region, but that of the detector is not assured.

The reference black body is a cylinder – type one. Temperatures of the interior surface of the blackbody are measured by a radiation pyrometer calibrated using the standard blackbodies at the National Research Laboratory of Metrology, Tokyo, Japan. Temperature of reference blackbody was controlled by utilizing the measured values of a thermocouple installed within the black body.

The intensity $v_B(\lambda_i, T_{Bj})$ of blackbody radiation at temperature T_{Bj} measured by the spectrophotometer at each wavelength λ_i is derived by the relation given in [9]

$$\varepsilon_N(\lambda_i, T_S) = \left[v_S - \frac{B(\lambda_i)}{C_2} \right] : \frac{A(\lambda_i)}{C_2} \quad (1)$$

$$e^{\lambda_i T_{Sroom}} - 1 \quad e^{\lambda_i T_S} - 1$$

where the second term does compensate the influence of ambient radiation at the room temperature. $A(\lambda_i)$ and $B(\lambda_i)$ are the measuring system constants that do depend upon the wavelength, and T_{Broomj} is the room temperature at the time of measurement at the blackbody temperature T_{Bj} . Intensity $v_B(\lambda_i, T_{Bj})$ at each wavelength λ_i is measured in advance at several temperatures T_{Bj} to determine the constants $A(\lambda_i)$ and $B(\lambda_i)$. Then, emittance of the specimen at temperature T_S , it can be set roughly, is calculated [9]

$$\varepsilon_N(\lambda_i, T_S) = \left[v_S - \frac{B(\lambda_i)}{C_2} \right] : \frac{A(\lambda_i)}{C_2} \quad (2)$$

$$e^{\lambda_i T_{Sroom}} - 1 \quad e^{\lambda_i T_S} - 1$$

where $v_S(\lambda_i, T_S)$ is the measured radiation intensity of the specimen layer, T_{Sroom} , room temperature at the time of the measurement. The measurement at each temperature is finished within several minutes. Temperatures of the

blackbody, specimen and room temperature do not change significantly during this period.

Total intensity $v_B^{\text{total}}(T_{Bj})$ measured by the total flux meter is described as in [9]

$$v_B^{\text{total}}(T_{Bj}) = A^{\text{total}} T_{Bj}^4 + B^{\text{total}} T_{Broomj}^4 \quad (3)$$

where A^{total} and B^{total} are constants of the total emittance measurement system. Intensity $v_B^{\text{total}}(T_{Bj})$ is measured in advance at several temperatures T_{Bj} for to determine the constants A^{total} and B^{total} . Total emittance of the specimen at T_S can be computed as in [9] by

$$\varepsilon_N^{\text{total}}(T_S) = \{ v_S^{\text{total}}(T_S) + B^{\text{total}} T_{Sroom}^4 \} / (A^{\text{total}} T_S^4) \quad (4)$$

where $v_S^{\text{total}}(T_S)$ is the measured total radiation intensity of the specimen layer, and T_{Sroom} is the room temperature at the time of the optical measurement.

3. RESULTS AND DISCUSSION

3.1 Total emittance of ash layers

Temperature dependence of total (hemispherical) emittance of the tested ash layers was analyzed. Both specimens (of $t=5 \text{ mm}$) were tested at 560-1460-560 K (heating + cooling, section 2.3). Two types of the total emittance were compared: $\varepsilon_N^{\text{total}}$, measured by the total flux meter, was compared to $\varepsilon_N^{2.5-25\mu\text{m}}$, computed from spectra of emittance ε_N (measured over $\lambda=2.5-25 \mu\text{m}$ in the present experiment) as in [9]:

$$\varepsilon_N^{2.5-25\mu\text{m}} = \frac{\int_{2.5\mu\text{m}}^{25\mu\text{m}} \varepsilon_N(\lambda, T_S) \cdot v_B(\lambda, T_S) d\lambda}{\int_{2.5\mu\text{m}}^{25\mu\text{m}} v_B(\lambda, T_S) d\lambda} \quad (5)$$

This integral-differential equation is solved as sum-difference equation by approximating integrals with sums, by using ‘‘trapezoidal rule’’ of numerical integration. Since > 95 % (75 %) of Planck black-body emission at 560 K (1460 K) lies within this wavelength region, total emittances $\varepsilon_N^{2.5-25\mu\text{m}}$ and $\varepsilon_N^{\text{total}}$ are well comparable. The temperature dependencies of both types of total emittance (of Specimen No.1) are shown in Figure 3.

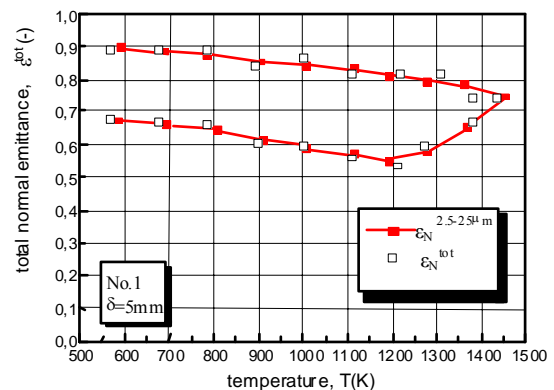


Figure 3. Total emittance vs. temperature of ash

It is obvious that the temperature dependences of $\varepsilon_N^{2.5-25\mu\text{m}}$ and $\varepsilon_N^{\text{total}}$ comply with each other. The same

conclusion holds for the Specimen No.2. This fact does indeed mutually confirm the validity of both conducted measurements: (a) using FTIR spectrophotometer and (b) using total radiation fluxmeter. Also, the comparison of Figure 3 and Figure 1, i.e. of the data from the present experiment and data of other authors, that obviously do comply well, additionally confirms this validity.

3.2 Emission spectra of ash layers

Figure 4 shows the spectra of the emissive power of thermal radiation flux of an ash deposit layer, within the narrow solid angle defined by a zenith angle of $\pm 10^\circ$. The spectra shown have been measured during the heating process within the 580-1460 K temperature interval, and represent an example of raw measurement data. Similar spectra have been gathered during the cooling part of the complete process, i.e. in the 1460-560 K interval. Both (heating- and cooling) spectra were measured in complete accordance with the methodology set in section 2.3, on Specimen No.1 (5 mm thick).

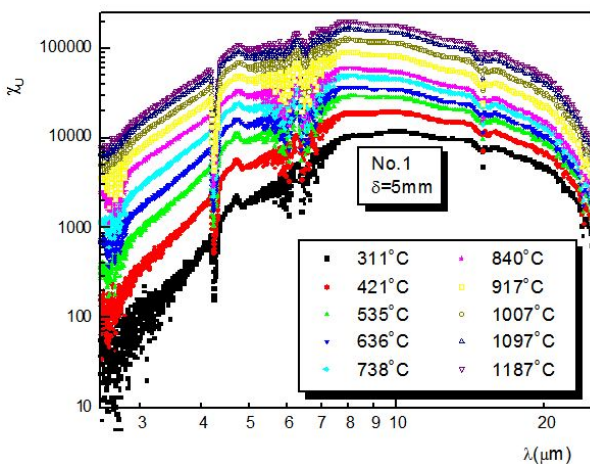


Figure 4. IR emissive power spectra of ash - heating

For clarity of the graphical representation, a common data reduction method has been used. The arithmetical mean of the emissive power values was determined, for each of the 1868 wavelength values, out of eleven (five – at left, one – central and five – at right) neighboring data points. After this data processing has been performed, the plot consists only of each 11th so-determined consecutive values. In that sense, for a specimen at certain temperature, only 187 data points are plotted instead of the multitude of 1868 data that are measured in the present experiments, by the FTIR spectrophotometer.

In the plot, one observes the influence of triatomic gases, present in the air above the heated specimen, that have the ability to absorb the radiation in certain intervals of wavelength (absorption bands) in the infrared spectral region. The carbon-dioxide and water-vapor absorption bands are pronounced in $\lambda = 2.6-2.7 \mu\text{m}$ range, absorption by only CO_2 in the bands about $\lambda = 4.3 \mu\text{m}$, and about $\lambda = 15 \mu\text{m}$, and absorption by only H_2O in the band about $\lambda = 6.3 \mu\text{m}$. Absorption by CO_2 exerts most critical distortive effect on the measurement results in the $\lambda=4-5 \mu\text{m}$ region, with high absorption peaks.

3.3 Emittance spectra of ash layers

Spectral emittances of the two ash deposit layers, in the direction perpendicular to specimen surface (within the solid angle defined by a zenith angle of $\pm 10^\circ$), during their heating in 560-1460 K range, during the complete experiment (560-1460-560 K) are shown in Figure 5 - left, for the two tested ash deposit specimens (No.1 and 4) of equal thickness ($t=5 \text{ mm}$). These values are determined by using the formulae (1) and (2) i.e. by properly following the methodological approach that is described in section 2.3.

One can observe that spectral emittance (at a constant temperature) continually increases with the wavelength in each spectrum. The increase is steep in the central part of each spectrum ($\lambda = 4-7 \mu\text{m}$). To the left and to the right from this interval, the emittance is practically constant, i.e. it is not sensitive to the change in wavelength. However, for λ lower than $4 \mu\text{m}$ – increase of emittance with the temperature is noticeable, while in $4-7 \mu\text{m}$ range the same dependence weakens with wavelength. Also, at values higher than $7 \mu\text{m}$ – isothermal lines of spectral emittance of ash deposits practically co-incide.

$$\varepsilon_H(\lambda) \cong \varepsilon_N(\lambda) = \frac{\varepsilon_{\min} + \varepsilon_{\max} (\lambda/\lambda_m)^p}{1 + (\lambda/\lambda_m)^p} \quad (6)$$

where: ε_{\min} , ε_{\max} are – the horizontal asymptotes of the fitting line i.e. emittance for $\lambda \rightarrow 0$ and $\lambda \rightarrow \infty$. Also, λ_m and p are, respectively: abscissa of the mid-point of the slope and – the slope power (exponent). Figure 5 - left represents the ash deposit emittance spectrum. Figure 5 - right shows the curve fits of these experimental spectra, as it is described in detail in section 4. The spectra of ash deposit emittance (and fits) for cooling of the Specimens No.1-4 (Figure 6) are of the same form like during heating. The emittance increases with temperature in $\lambda=2.5-4 \mu\text{m}$ range, but all lines (for constant temperatures) are noticeably higher. This “hysteresis” tendency is a direct consequence of the irreversible physical and chemical changes those occurring during the processes of sintering and fusion (melting) of ash deposits above 1200 K.

4. EXPERIMENTAL DATA CORRELATION

To solve the radiation heat transfer in a power boiler accurately, under sharp temperature distribution, spectral analysis is recommended today [8,9,10] as it was two decades ago [11]. That is so because using the emittance spectra of ash layers is more adequate than the traditional total analysis, using those of total emittance. Of course, emittance used in the classical radiation energy exchange calculations, using the view factors, is the hemispherical emittance ε_H , that is not identical to the normal emittance ε_N of the present measurement. But, as mentioned earlier, directional characteristics of the emittance are weak [3], and thence the values of ε_N are considered close enough to those of ε_H . This is a vital issue since, clearly, it is much simpler (and cheaper) to measure the emissive power in normal direction than – into hemisphere.

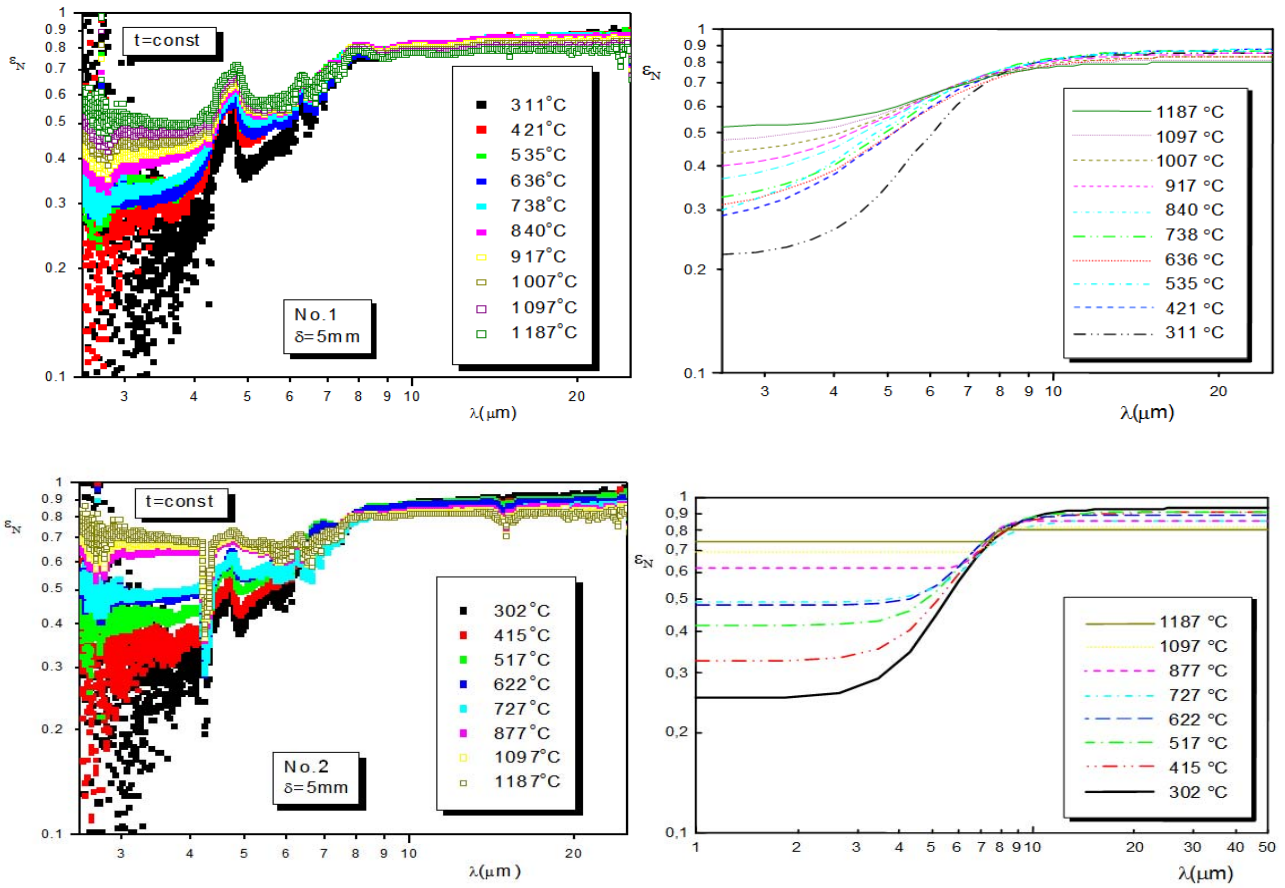


Figure 5. Spectra of ash deposit emittance in heating mode (left=experiment; right=fit)

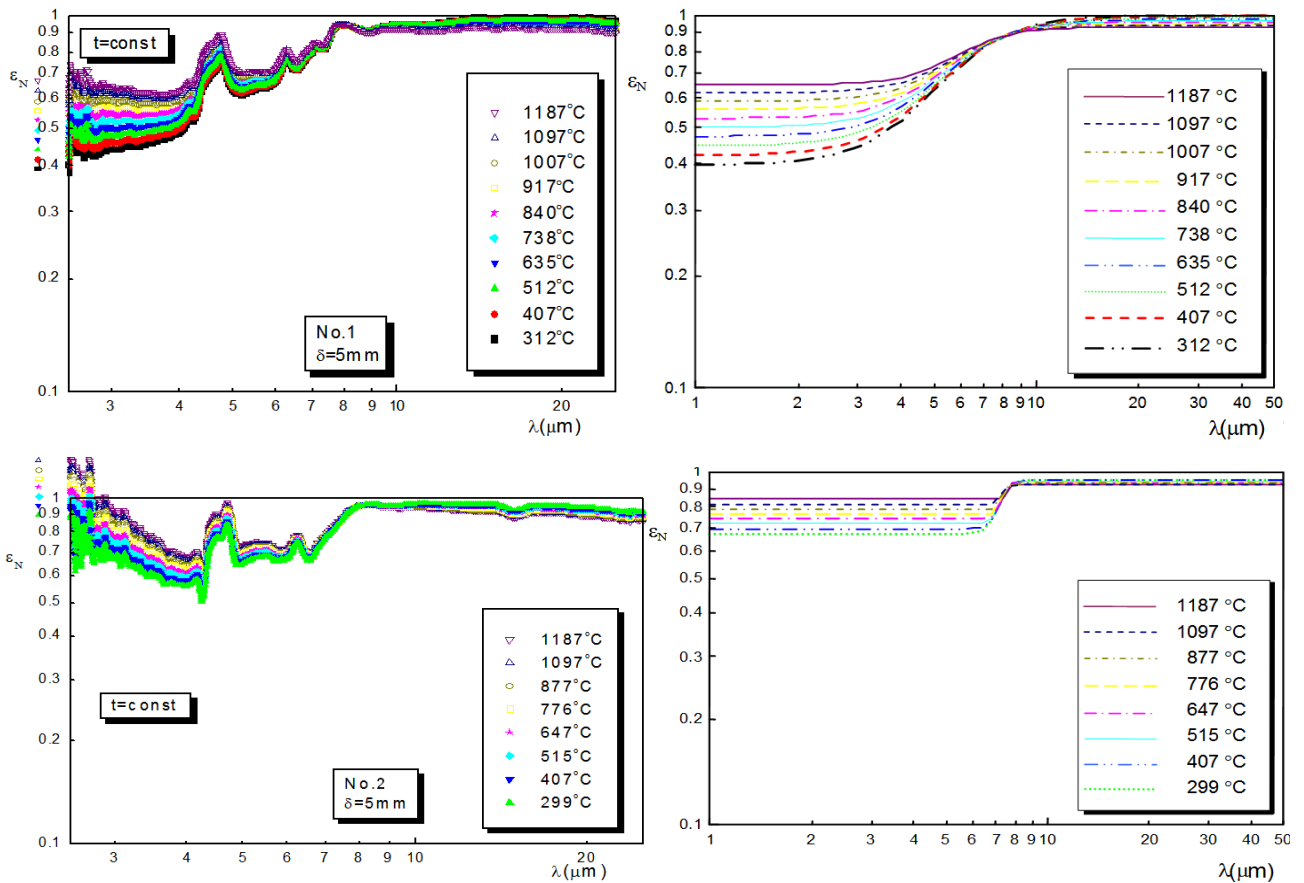


Figure 6. Spectra of ash deposit emittance in cooling mode (left=experiment; right=fit)

Table 3. Parameters: $\varepsilon_{min}(T)$, $\varepsilon_{max}(T)$, $p(T)$ and λ_m , of the function $\varepsilon_H(\lambda, T)$

HEATING	COOLING
Sample No 1	
$\varepsilon_{min} = -0,95345 + 0,18209 \ln T$ $\varepsilon_{max} = 0,76141 + 0,01395 \ln T$ $\lambda_m = 5,74454$ $p = 10,10669 - 0,8913 \ln T$	$\varepsilon_{min} = 0,28924 + 0,01473 \ln (T - 565)$ $\varepsilon_{max} = 1,77634 - 0,12915 \ln T$ $\lambda_m = 5,3425$ $p = 4,20326 + 0,05246 \ln (T - 565)$
Sample No 2	
$\varepsilon_{min} = -2,95693 + 0,50416 \ln T$ $\varepsilon_{max} = 1,64314 - 0,11198 \ln T$ $\lambda_m = 6,55818$ $p = -238,44449 + 32,0406 \ln (T + 1317)$	$\varepsilon_{min} = 1,17802 - 0,08626 \ln (T - 412,75833)$ $\varepsilon_{max} = 6,10311 - 0,65156 \ln (T - 20233,123)$ $\lambda_m = 7,22836$ $p = 203,08212 - 26,46075 \ln T$

For an actual engineering application, it is desirable that ε_H spectrum is in a form of a continuous function of radiation wavelength λ and temperature T . This adds to the extrapolation of the wavelength region and – also to the convenience of the numerical computation. We have proposed the function (6) to correlate the experimentally determined points. The empirical curves, shown in Figure 5 - left and 6 - left, were treated by a best-fit method – to solve for the parameters. Table 3 presents the result of performed research – the obtained temperature dependent correlations: $\varepsilon_{min}(T)$, $\varepsilon_{max}(T)$ and $p(T)$ for the two tested specimen layers (heating + cooling) that are usable in the thermal design of the very furnace where the samples are taken from, however as well in the thermal design of the similar furnaces using same type of coal.

The figures 5 – right and 6 – right, are the curve fits obtained by fitting measurement results by the function of simple visual and analytical form, as defined by equation (6). It presents the chosen functional dependence of the spectral emittance upon wavelength and temperature: $\varepsilon_H \approx \varepsilon_N(\lambda, T)$. The same figures contain curves fitted – for each temperature separately – during heating and cooling. The lines are extrapolated beyond the wavelength region of the experiment. However, in the far-infrared region up to several ten μm , in wavelength, outside the experimental region, various lattice vibration modes in the complex inorganic crystals in the ash are distributed all over the region, and strong absorption with higher emittance is preserved here. In the near-infrared region outside the present experiment, the shorter wavelength tail of the Planckian energy distribution to be multiplied with the emittance is low enough, and thus the crude assumption of the emittance in this region, does not exert any significant effect on the computed energy flux.

Table 3 contains the recommended formulae of temperature dependent functions: $\varepsilon_{min}(T)$, $\varepsilon_{max}(T)$ and $p(T)$. Parameter λ_m is (obviously) not too sensitive to temperature changes, thus, its mean value can be used, for simplicity. A rough analysis of the data suggests that: (A) the empirical correlations for $\varepsilon_{min}(T)$, $\varepsilon_{max}(T)$, $p(T)$ and λ_m – related to deposit heating - can be used only for furnace parts with lower temperatures, where sintering does not occur; and (B) for the furnace sections with well higher temperatures, where sintering does occur, the empirical correlations for $\varepsilon_{min}(T)$, $\varepsilon_{max}(T)$, $p(T)$ and λ_m should be taken solely from the tables related to deposit cooling.

This method can be extended to the other specimens from the same furnace. For each zone of the furnace, that is being thermally designed, appropriate correlations shall be used. The results i.e. obtained data are applicable to thermal design of new furnaces - with similar geometry and combusting similar coal - as the existing ones.

However, the proposed method is applicable more generally. It could be used even in the cases with totally different boiler furnaces combusting completely different coal. One should just run the whole experiment again but with own - new ash deposit samples. The newly derived data will then be applicable to the thermal design of those new furnaces – having similar geometry and combusting similar coal as in these new experiments.

5. CONCLUSIONS AND RECOMMENDATIONS

In order to facilitate the computation of the energy transfer in coal combustion boilers of power plants, with strong fouling (ash depositions), investigation was done (by present authors) on infrared radiation characteristics of coal ash layers. The obtained results were discussed and analyzed from an engineering point of view.

The concluding remarks have been summarized in the following statements:

- spectral normal emittance continually increases with the increase of wavelength, as well as with the increase of temperature, especially at lower wavelengths;
- above 1200 K ash layers are sintered and fused, and higher density layers are formed that can't possibly reach their initial state by any cooling;
- total emittance decreases with rise of temperature to the onset of sintering, then increases to the onset of fusion, and in the cooling mode a “hysteresis” is present;
- value of ε_N in the $\lambda = 2.5\text{-}4 \mu\text{m}$ wavelength region in the cooling mode is higher than that in the heating mode, as a consequence of ash sintering and – fusion;
- we propose to correlate the experimentally obtained emittance spectra with one continuous function, equation (6), that defines the dependence of ε on λ and T ;
- we do suggest a selective use of the temperature dependent parameters in equation (6): $\varepsilon_{min}(T)$, $\varepsilon_{max}(T)$, $p(T)$ and λ_m ; those bound with the “heating” data – only for furnace sections with low temperature (where

deposits can not sinter), and those bound to the “cooling” data for furnace sections with high temperature (deposits sinter);

- this technique can be extended to other specimens from the same boiler furnace; the obtained data are well applicable to thermal design of new furnaces with similar geometry and combusting similar type of coal - as in the existing boiler furnaces.

- the here proposed method is applicable even more generally; with different boiler furnaces combusting a different coal; the experiments should be run onto own - new deposit samples; data will be applicable to thermal design of new classes of furnaces, with similar geometry and combusting similar coal, as in these new experiments.

REFERENCES

- [1] Mulcahy, M.F.R., Boow, J. and Goard, P.R.C.: Fireside deposits and their effect on heat transfer in pulverized- fuel boiler: part I, Journal of Institute of Fuel, Vol. 39, pp. 385-394, 1966.
- [2] Mulcahy, M.F.R., Boow, J. and Goard, P.R.C.: Fireside deposits and their effect on heat transfer in pulverized- fuel boiler: part II, Journal of Institute of Fuel, Vol. 39, pp. 394-398, 1966.
- [3] Wall, T.F., Bhattacharya, S.P., Zhang, D.K., Gupta, R.P. and He, X.: The properties and thermal effects of ash deposits in coal-fired furnaces, Progress in Energy and Combustion Science, Vol.19, pp. 487-504, 1993.
- [4] Goodwin, D.G.: Infrared Optical Constants of Coal Slags, PhD Thesis, School of Mechanical Engineering, Stanford University, Palo Alto, CA, 1986.
- [5] Bhattacharya, S.P., Wall, T.F. and Arduini-Schuster, M.: A study on the importance of dependent radiative effects in determining the spectral and total emittance of the ash deposits in pulverized fuel furnaces, Chemical Engineering and Processing, Vol. 36, pp. 423-432, 1997.
- [6] <http://www.ssi.shimadzu.com/products/>
- [7] [<http://www.se.konicaminolta.us/products/>]
- [8] Zbogar, A., Frandsen, F.J., Jensen, P.A. and Glarborg, P.: Heat transfer in coal ash deposits: a modelling tool-box, Progress in Energy and Combustion Science, Vol. 31 pp. 371-421, 2005.
- [9] Vučićević, B.: Prilog Rešavanju Problema Određivanja Ukupne Polusferne Emisivnosti Naslaga Stvorenih pri Sagorevanju Domaćih Lignita, Master's thesis, Faculty of Mechanical Engineering, Belgrade University, Belgrade, SRB, 2004. (in Serbian)
- [10] Itaya, Y., Nishio, N., Hatano, S., Kobayashi, N., Mori, S. and Kobayashi, J.: Near- infrared radiation and scattering properties of coal fly ash particles cloud, Journal of Chemical Engineering of Japan Vol. 39, No. 7, pp. 718-723, 2006.
- [11] Baxter, L.L., Fletcher, H.T. and Ottesen, D.K., Spectral emittance measurements of coal particles, Energy and Fuels, Vol. 2, pp. 423-430, 1988.

NOMENCLATURE

A, B	system constants for optical measurements
C2	Planck's 2nd radiation constant (=0.014388 m·K)
p	slope of the inclined part of the fitting line
t	thickness of specimen layer, m
T	temperature, K

Greek symbols

ε	radiation emittance
$\varepsilon_{\max}, \varepsilon_{\min}$	emittance asymptotes of the fitting line
λ	wavelength of radiation, μm
λ_m	wavelength of mid-slope of the fitting line, μm
ν	output of optical measurement system
ρ_p	heaping mass density of specimen layer, kg/m^3

Subscripts

B	blackbody
H	hemispherical
i(j)	corresponding to wavelength (temperature)
N	normal
room	room temperature
S	specimen

Superscripts

2.5-25	spectrally-integrated over $\lambda=2.5-25$
μm	μm
total	over the whole spectrum

ИСТРАЖИВАЊЕ ИНФРАЦРВЕНОГ СПЕКТРА ЕМИСИЈЕ НАСЛАГА ПЕПЕЛА УГЉЕНОГ ПРАХА

**А. Салњиков, М. Гојак, М. Трифуновић,
С. Андрејевић, М. Добрњац**

У овом раду се описује истраживање спектралних и тоталних емисивности топлотног зрачења наслага пепела угљеног праха у ложиштима термоелектрана. Спектри нормалне емисивности у интервалу таласне дужине 2.5-25 μm , те тотална нормална емисивност, су измерени на два узорка спрашеног пепела у слоју дебљине реда величине mm, на 560→1460→560 K у току загревања и – хлађења. Спектрална емисивност расте са порастом температуре као и таласне дужине зрачења пепела. Спрашени пепео се синтерује и топи на температури над 1200K. Емисивност синтерованог пепела је већа од емисивности несинтерованог праха.

Аутори предлажу, наводећи један конкретан пример, корелисање експериментално добијених

спектралних емисивности наслага пепела, континуалним кривама чије формуле дефинишу зависности емисивности од таласне дужине и температуре т.ј. $\varepsilon = \varepsilon(\lambda, T)$. Може се очекивати да ће коришћење предложене формуле, уз вредности

параметара одређене помоћу предложеног поступка, у великој мери поједноставити практичну примену експериментално одређених емисивности у оквиру топлотног прорачуна постојећих као и нових ложишта парних котлова на угљени прах.